

Visual Analytics of Multivariate Networks with Representation Learning and Composite Variable Construction

Hsiao-Ying Lu, Takanori Fujiwara, Ming-Yi Chang, Yang-chih Fu, Anders Ynnerman, and Kwan-Liu Ma

Abstract—Multivariate networks are commonly found in real-world data-driven applications. Uncovering and understanding the relations of interest in multivariate networks is not a trivial task. This paper presents a visual analytics workflow for studying multivariate networks to extract associations between different structural and semantic characteristics of the networks (e.g., what are the combinations of attributes largely relating to the density of a social network?). The workflow consists of a neural-network-based learning phase to classify the data based on the chosen input and output attributes, a dimensionality reduction and optimization phase to produce a simplified set of results for examination, and finally an interpreting phase conducted by the user through an interactive visualization interface. A key part of our design is a composite variable construction step that remodels nonlinear features obtained by neural networks into linear features that are intuitive to interpret. We demonstrate the capabilities of this workflow with multiple case studies on networks derived from social media usage and also evaluate the workflow through an expert interview.

Index Terms—Interpretability, network representation learning, composite variable, density scatterplots, neural networks, visualization.

1 INTRODUCTION

Multivariate networks [36] consisting of both topological and semantic information can model complex relations between entities. One common analysis task performed on multivariate networks is to understand associations among structural and semantic characteristics [3, 12, 13, 36]. For example, from social media usage, analysts may want to see how likely each possible combination of individual characteristics (e.g., age, gender, and extraversion) and friendship structures is related to their addiction level to social media. Such analysis can be very complicated when the associations underlie intertwining social facts.

To aid in analysis of multivariate networks, researchers have introduced visual analytic support, including network layouts considering semantic information, interactive simplification, and incorporation of coordinated views [36, 55]. Among others, utilizing network representation learning (NRL) [33, 78] is one promising approach as it can capture latent features of networks and highlight essential aspects that should be examined with visualizations. Existing visual analytics methods [23, 24, 48, 49, 64, 68] utilize NRL methods to learn networks' general representations—overall summaries of networks (e.g., variance of node degrees). However, to identify associations, a general-purpose NRL is not effective as it is not particularly designed to capture latent features important for associations of interest.

On the other hand, as seen in the machine learning field, NRL using neural networks (NNs) can learn representations specific to an analysis focus by using appropriate loss functions [29]. While these representations are suitable for fully automated analyses, such as network classification, it is often difficult for analysts to interpret the extracted features. This is not preferable when analysts want to be involved in the analysis process and derive insights into associations.

To address the aforementioned problems, we introduce a visual analytics workflow that provides (1) network representations specific to the structural and semantic associations in multivariate networks as well as (2) interpretation supports for the analysis results.

- Hsiao-Ying Lu and Kwan-Liu Ma are with University of California, Davis. E-mail: {hyllu, klma}@ucdavis.edu.
- Takanori Fujiwara and Anders Ynnerman are with Linköping University. E-mail: {takanori.fujiwara, anders.ynnerman}@liu.se.
- Ming-Yi Chang is with Fu Jen Catholic University. E-mail: mychang@mail.fju.edu.tw.
- Yang-chih Fu is with Academia Sinica. E-mail: fuyc@gate.sinica.edu.tw.

Manuscript received xx xxx. 201x; accepted xx xxx. 201x. Date of Publication xx xxx. 201x; date of current version xx xxx. 201x. For information on obtaining reprints of this article, please send e-mail to: reprints@ieee.org. Digital Object Identifier: xx.xxx/TVCG.201x.xxxxxxx

To learn such representations, we first extract essential structural features by using an NRL method and then train an NN model that is designed to classify values of a user-selected attribute (e.g., high and low addiction levels to social media). After training, the model generates latent features that are highly related to the selected attribute.

For the interpretation of the obtained network representations, we employ dimensionality reduction (DR), interactive visualization, and composite variables [65]. To help analysts assess the quality of the representations, we simplify the latent features with a linear DR method (specifically, linear discriminant analysis or LDA). We then visualize the information of the simplified features in a 2D plot, where the distribution of networks or their elements (i.e., nodes and links) is shown along a latent direction that is related to the classification. From this plot, analysts can judge which part of networks or elements (e.g., subjects with age 20–30) likely holds clearer associations with the selected attribute. This analysis is almost infeasible if we rely only on the classification quality measures. In addition, we introduce a mechanism of composite variable construction to explain the meanings of the network representations. The mechanism first suggests network structures and attributes highly related to the representations by utilizing a model-agnostic interpretation method, the SHAP [46]. Then, after analysts interactively select structures and attributes from the suggestion, an optimization method automatically generates a composite variable that resembles the network representation. By examining this composite variable, analysts can understand the associations among the selected attributes and the other information.

To support effective analysis of the associations, we develop a new density scatterplot, named *two-class density scatterplot*, that can clearly depict a trend of data distribution as well as inform the mixture and separation of two classes. Incorporating two-class density scatterplots, we develop an interactive interface that links visualizations designed to enhance the visual analytics workflow. We further demonstrate the capabilities of the workflow and interface with three case studies using two real-world datasets on social media usage. Moreover, we validate the usability of the workflow through an expert interview.

In summary, we consider our primary contributions to be:

- a visual analytics workflow considering both generation and interpretation of network representations that are expressive for user-specified analysis targets;
- a mechanism of composite variable construction that aids in attribute selection and attribute weight optimization for interpretations with an influence from multiple attributes; and
- a two-class density scatterplot as a versatile visualization to review individual- and group-level data patterns with class information.

We provide source code related to the workflow and a demonstration video of interactive analysis [1].

2 RELATED WORK

Our work is closely related to two topics in the visualization field: NRL and the interpretation of learned representations. For the broader discussion on visualizations for analyzing networks and interpreting machine learning results, refer to existing surveys [5, 10, 36, 51].

2.1 Learning Network Representations

NRL aims to generate a set of low-dimensional vectors (also called representation) that captures certain important characteristics of networks, nodes, or links [78]. The representation is usually learned for downstream tasks, such as node classification and link prediction. Various NRL methods are developed, including node2vec [27], graph convolutional networks [37], graph neural networks (GNNs) with the self-attention [76], to name but a few [78].

The researchers have been utilizing NRL for visualization to interactively examine complex network datasets. For example, Freire et al. [19] represented one network by a set of network statistics (e.g., degree distribution) to compare many networks in a tabular interface. Gove [26] suggested several network-level features (e.g., density) that are easier to interpret and faster to compute for interactive visualization. Other researchers utilized the occurrences of graphlets [60] (small, connected, non-isomorphic subgraph patterns in a network) to identify visually similar networks [31, 40, 71]. When node correspondence exists among networks, another common approach is directly applying DR methods to networks' adjacency matrices to capture the similarities of networks [4, 20]. Van den Elzen et al. [68] took a similar DR approach while further incorporating network statistics. Martins et al. [48, 49] used DR to lay out nodes by their structural and semantic similarities.

Similar to ours, recently, a few works employed NN-based NRL. Fujiwara et al. [24] introduced contrastive NRL (cNRL) by integrating a variant of GNNs and contrastive learning [82]. cNRL extracts a representation of two networks, where salient characteristics in one network relative to another are highlighted. Utilizing linear DR, they further designed an interpretable cNRL method and enhanced it with interactive visualizations [23]. Song et al. [64] used GNNs to support interactive subgraph pattern search, where GNNs are used to covert each network in a comparable, fixed-length latent vector.

Unlike the above approaches, we use NN-based NRL to obtain representations that are specifically for uncovering the associations of interest in multivariate networks. Also, we address the interpretation of network representations with composite variable construction, which is easier to understand when compared with the approaches referring to complex coefficients in linear DR results [23, 24].

2.2 Interpreting Representations

Although the interpretation support for NRL is still sparsely studied (e.g., [23]), a set of interpretation methods are developed for representations of high-dimensional data. Such representations are often extracted by DR methods or NNs [33]. Existing interpretation methods can be categorized into two approaches: (1) identifying essential information to specific patterns found in representations (i.e., post-hoc explanation approach) and (2) constructing simple, interpretable representations during a learning phase (i.e., explainability-by-design approach [30]).

Many visual analytics methods for the interpretation of nonlinear DR results fall under the first approach. For instance, researchers identified influential attributes on the cluster formation in DR results from statistical charts (e.g., boxplots of attributes for each cluster) [39, 53, 69]. As univariate statistics are often insufficient to capture the cluster characteristics, researchers further considered influences from multiple attributes [21, 35, 67, 77, 79]. For example, Joia et al. [35] applied PCA to each cluster to examine multivariate influences. Although many methods are designed to understand clusters, several methods are to understand other patterns (e.g., local correlations) [8, 11, 18].

There are a relatively small number of visual analytics works taking the explainability-by-design approach. Knittle et al. [38] used NNs consisting of one hidden layer with a small number of NN nodes to extract nonlinear representations that relate input attributes to a target output attribute. This simple NN allows analysts to identify a small number of representations that show clear associations between the input and target attributes. Gleicher [25] produced simple composite

variables that are to classify a user-selected attribute. To craft such composite variables, Gleicher performed a support-vector machine-based exhaustive search for the selection of composing variables while considering a balance between their simplicity and expressiveness.

In terms of using NNs to extract the input-output relationships, the work by Knittle et al. [38] is closely related to ours. However, their interpretation of the obtained representations is based only on univariate value distributions, which is insufficient when NNs capture complex input-output relationships. Similar to Gleicher's work [25], our work crafts simple composite variables, but we do not involve the computationally expensive exhaustive search. Instead, we rank variables based on their contributions to the NNs' predictions and involve analysts' knowledge to select attributes of interest.

3 METHODOLOGY

This section introduces our visual analytics workflow and two-class density scatterplot. We first describe design considerations of the workflow, which we identify based on our literature survey in Sec. 2 and targeted analysis on multivariate networks. We then provide an overview of the workflow, followed by the details of each step.

3.1 Design Considerations

The following five design considerations (DCs) are identified to support the analysis task for understanding associations of interest and to fill the analytical gap that is not covered by existing methods.

DC1: Flexibility. Analysis of multivariate networks requires reviewing intertwined relationships in both structural and semantic information [36]. Also, based on analysis purposes and available datasets, analysts often want to investigate networks from different levels, such as node, link, and network levels (e.g., node: [23, 49]; link: [14]; and network levels: [19, 40, 64, 68]). The workflow should provide flexibility to conduct analyses from multiple aspects at various levels.

DC2: Expressivity. Our work's main objective is to support examining associations among target (e.g., the addiction level to social media) and other related information (e.g., gender, age, and friendships). The workflow should be able to extract features that are expressive for this analysis task (i.e., containing important information to reveal associations) rather than providing a general summary of networks.

DC3: Interpretability. Interpretation is essential to gain insights into analysis results [25, 38]. Because expressive features such as those extracted by NNs are often difficult to interpret only from each individual attribute's influence [16, 23], the workflow should provide more advanced interpretation support that considers the combined influence from multiple attributes.

DC4: Tunability. Conflict often exists between the expressiveness and interpretability of features (i.e., more expressive, more difficult to interpret) [25, 47, 81]. Also, the required preciseness of interpretation can be varied by analysis (i.e., complicated but precise interpretation vs. less precise but simpler interpretation). The workflow should allow control of the balance of expressiveness and interoperability.

DC5: Extensibility. Although we provide a concretized method for each step of the workflow, a different set of methods may be more suitable according to the characteristics of future datasets and analysis goals [15, 22, 75, 78]. The workflow should be extensible to incorporate new or different methods.

3.2 Workflow Overview

Fig. 1 shows our workflow for reviewing associations embedded in multivariate networks. It consists of six steps that are performed first with a script for machine learning (Steps 1–4) and then with our user interface (UI) designed for visual analysis (Steps 5–6). The UI is shown in Fig. 2. As we describe in Sec. 3.5, we extract structural information as a set of network measures (e.g., degree and betweenness centralities) for each element (i.e., node, link, or network); thus, in the following, we use a term, attribute, to indicate both extracted structural (e.g., degree) and semantic information (e.g., age).

Step 1. The workflow begins with the extraction and selection of input attributes and one output/target attribute. For example, to know how students' grades in a school class are related to their surrounding conditions, an analyst can choose their attending class size, mental

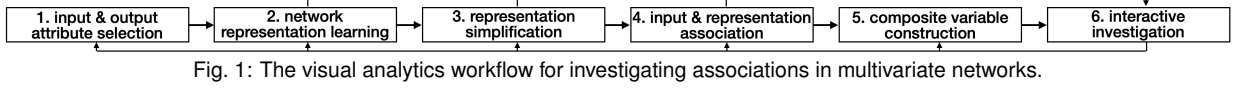


Fig. 1: The visual analytics workflow for investigating associations in multivariate networks.

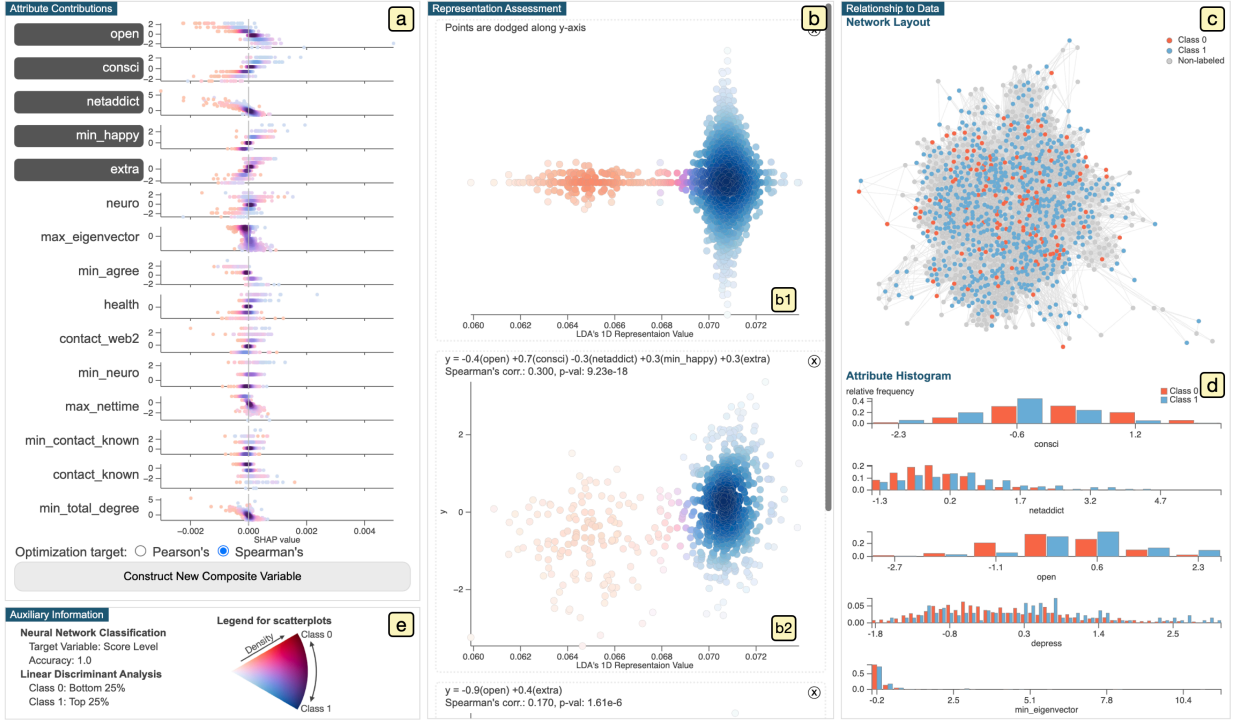


Fig. 2: The visual interface for facilitating interactive analysis using the workflow in Fig. 1. (a) Relating to Step 4, this view visualizes input attributes' contributions to the 1D network representation. (b) Composite variables generated in Step 5 are shown as a list of scatterplots, where the 1D network representation and composite variable correspond to x- and y-axes, respectively (see b2). As shown in b1, when a composite variable is not generated yet, a swarm-plot-like visualization presents the 1D network representation generated through Step 3 to help assess its quality. For a and b, we employ our two-class density scatterplots. (c) A node-link diagram and (d) a set of histograms inform the network structure and attribute distributions. (e) Other auxiliary information is displayed, including the prediction accuracy of NNs trained for Step 2.

health status (e.g., depression level), and centrality in social media connections (e.g., degree) as inputs and their grade as an output.

Step 2. NRL is performed based on the selected inputs and output. A network representation is generated by an NN trained to perform binary prediction of the output (e.g., good or bad grade) with the inputs. The derived representation directly relates to associations of interest.

Step 3. This step compresses the dimensionality of the network representation into one while preserving the prediction quality as much as possible. This makes the remaining steps simpler to complete and the related results easier to interpret.

Step 4. This step evaluates and ranks each input attribute's contribution to the 1D compressed representation. The obtained ranks can be considered as recommendation levels for the inclusion of the corresponding attributes for composite variable construction in Step 5.

Step 5. Finally, based on the recommendation levels and interests, an analyst manually selects a small set of attributes (e.g., 2–5 attributes) and runs a composite variable construction algorithm. The optimized composite variable (e.g., y-axis in Fig. 2-b2) maximally resembles the 1D compressed representation (e.g., x-axis in Fig. 2-b2). This composite variable provides an intuitive explanation of how the selected small set of attributes is related to the output/target attribute.

Step 6. The UI in Fig. 2 visualizes the information related to each previous step as well as the detailed structural and semantic information of the multivariate network. By interactively reviewing visualizations, the analyst can gain insights or adjust settings for each step based on their need (the backward arrows in Fig. 1).

3.3 Two-class Density Scatterplot

We here introduce a *two-class density scatterplot* (Fig. 3-d), which we use to visualize results from most of the steps in the workflow. From a scatterplot of two variables (e.g., the 1D compressed representation and

the composite variable generated at Steps 4–5), we aim to simultaneously depict (1) patterns related to binary classes; (2) trends including correlations; (3) other supplemental patterns, such as noises, outliers, and clusters. For example, analysts may want to review class separation to assess the quality of network representations, correlation patterns related to the composite variable to gain insights, and patterns only seen in subgroups to consider further analyses.

According to a survey on scatterplot designs [63], we should employ an aggregated-level visual encoding (e.g., binning-based encoding) of instances to reveal trends while we should show individual instances for the other tasks (e.g., finding outliers). However, designing an encoding that satisfies these requirements is not straightforward. For example, in Fig. 3-a, class information is encoded with colored dots. This encoding easily suffers from overplotting when analyzing a large dataset (e.g., 1000 instances). In Fig. 3-a, it is difficult to find a clear trend due to noises. In contrast, density scatterplots are effective in finding trends. For instance, Fig. 3-b reveals a correlated pattern. However, from density scatterplots, we cannot grasp distributions related to classes (e.g., whether the dense area mostly consists of a single class). A few existing scatterplot enhancements, splatterplots [50] and winglets [44], can show both aggregated- and instance-level information along with class information. However, based on our experiment [1], both enhancements still easily suffer from overplotting and noises. Also, these enhancements are sensitive to the choice of parameters of their algorithms (e.g., threshold for contouring) and visualizations (e.g., dot size).

A two-class density scatterplot (Fig. 3-d) is designed to solve the above issues. Using a bivariate colormap, a two-class density scatterplot encodes the *total density* from both classes and the *density ratio* of each class with color lightness and hue, respectively. In Fig. 3-d, first, we can clearly see the correlated pattern as in the density scatterplot. In addition, we can confirm that two dense areas at the bottom left

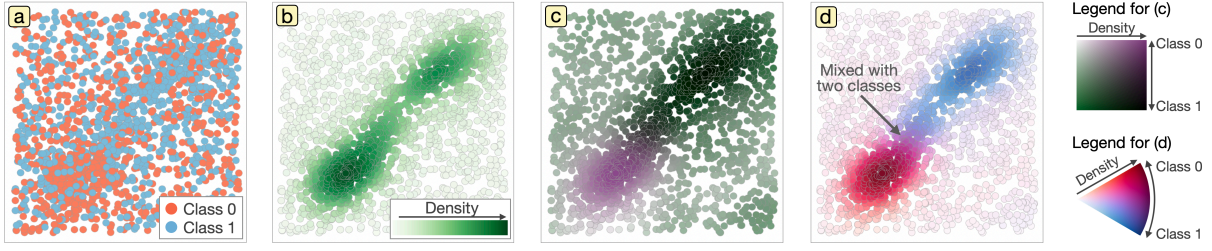


Fig. 3: The comparison of scatterplot designs: (a) scatterplot with colored classes, (b) density scatterplot, (c,d) scatterplots encoding the total density and the ratio of each class’s density with two different bivariate colormaps. (d) is our final design for a two-class density scatterplot.

(more red colors) and top right (more blue colors) mainly consist of a single class. Moreover, from the purple-color area annotated with the arrow, we can observe that a part of the dense areas mixes a considerable amount of both classes’ instances. We should note that a bivariate colormap has been already utilized to simultaneously show two different measures over scatterplots (e.g., [42]). Our contribution is in the computation of the ratio of each class’s density and the color encoding design that is suitable to depict class and density information with scatterplots.

Computation of density-related information. Similar to an ordinary density scatterplot, we first estimate a 2D probability density function (PDF) from the coordinates of instances. To obtain a PDF, we apply a Gaussian kernel density estimation to all instances. Let f_{all} denote a 2D PDF estimated with all instances (i.e., the total density). Then, the density at a 2D coordinate, \mathbf{p} , can be computed with $f_{\text{all}}(\mathbf{p})$. Similarly, let f_0 and f_1 denote 2D PDFs estimated with Class 0’s instances and Class 1’s instances, respectively. Also, let n_0 and n_1 be the numbers of instances in Class 0 and Class 1. Then, a function that estimates the density ratio of Class 0 at \mathbf{p} can be written as: $g_0(\mathbf{p}) = n_0 f_0(\mathbf{p}) / (n_0 f_0(\mathbf{p}) + n_1 f_1(\mathbf{p}))$. If assigning the same total density for each class is more appropriate for an analysis, we can use $g_0(\mathbf{p}) = f_0(\mathbf{p}) / (f_0(\mathbf{p}) + f_1(\mathbf{p}))$, instead.

Visual encoding design. Using a bivariate colormap, we encode $f_{\text{all}}(\mathbf{p})$ and $g_0(\mathbf{p})$. We select color lightness to encode the total density, $f_{\text{all}}(\mathbf{p})$, because of its natural metaphor: the more accumulation of dots, the denser color. We then employ hue to represent the density ratio, $g_0(\mathbf{p})$. To use lightness and hue, we initially used ordinary color spaces such as HSL; however, a subtle difference in the density was difficult to recognize from the generated colors. Thus, we decided to utilize existing carefully designed sequential colormaps. Specifically, we use the red and blue sequential colormaps in Matplotlib [66]. We can obtain a pair of colors corresponding to $f_{\text{all}}(\mathbf{p})$ from these two colormaps and then generate a linearly interpolated color from the pair based on $g_0(\mathbf{p})$. To show this 2D color space as a legend, we use a polar coordinate (see Fig. 3). This is to clearly indicate the difference between the meanings of two measures (total density and ratio) as well as to inform that the ratio difference is less emphasized in low total-density areas. As shown in Fig. 3-c, we also tested existing bivariate colormaps such as one introduced by Lespinats and Aupetit [42]. This colormap was not suitable for two-density scatterplots. For example, it is difficult to recognize Class 1’s high-density area and the density difference between the high-density areas of Class 0 and Class 1.

3.4 Datasets: Students and Adults’ Network Resources

In the rest of this section, our explanations refer to a real-world dataset, Dataset I, as a concrete analysis target. In addition to this dataset, we also analyze DatasetII in our case studies (Sec. 4). Both datasets are derived from the Facebook usage and survey data of representative cohorts in Taiwan. While Dataset I is a single multivariate network, Dataset II consists of a set of egocentric multivariate networks.

Dataset I is about senior college students [9]. We represented each student as a network node and created a link based on their interactions on Facebook. We constructed an undirected link if a “like”, “comment”, or “tagged” was made between students on a post. We consider such links as “friendships” in social media and 1-hop neighbors of each node as “friends”. We further used the answers for the survey as each node’s attributes. The corresponding questions are related to the

students’ school life, such as their personalities, moods, and grades. The resultant network consists of 1886 nodes, 64156 links, and 226 survey-based attributes for each node.

Dataset II is collected from sampled adults [41]. This dataset uses Taiwan Social Change Survey, which includes important network-related topics, such as core discussion networks and network resources, as well as personal attributes, such as their backgrounds, personalities, moods, and social lives. We generated multivariate egocentric networks by adding 1- and 2-hop neighbors of each survey respondent based on their contact records (i.e., 1-hop: direct contacts, 2-hop: indirect contacts). We also assigned network-level attributes, such as the ego node’s personality, Facebook usage statistics, and network measures (e.g., clustering coefficient). The resultant egocentric networks consist of 345 ego nodes, 3339 1-hop neighbors, 19917 2-hop neighbors, and 11 network-level attributes. In addition, we have information about whether each indirect contact is promoted to direct during a study period, January 1, 2015–June 30, 2017.

Below, from Dataset I, we identify and review college students’ attributes that are highly related to their `scorelevel1`—the past three years’ mean score levels reported on a scale of four from the top to bottom. We used 14 survey attributes related to this analysis.

3.5 Learning Representations

We explain Steps 1–3, where we learn representations from multivariate networks. To provide a concise explanation, here we describe each process for producing a latent vector of each node (i.e., node feature learning). However, the described learning processes can be easily adjusted to learn a latent vector for each link or network (DC1: Flexibility). Sec. 4.3 demonstrates a case for network feature learning.

3.5.1 Structural Feature Extraction for Attribute Selection

To select attributes related to the structural information in Step 1, we first precompute a set of structural measures [23, 68]. For node feature learning, such measures can be degree, eigenvector, betweenness centralities, and many others [54].

These centralities inform the importance of each node from different aspects. Degree centrality (i.e., the number of links connected to a node) measures local importance of nodes in the network. Eigenvector centrality (i.e., the eigenvector corresponding to the greatest eigenvalue of the network’s adjacency matrix) more reflects global importance of nodes than degree centrality. This is because eigenvector centrality considers the transitive importance of links (e.g., a link to a node with 100 links is more important than one with 1 link). Betweenness centrality (the number of shortest paths that pass through a node) indicates a node’s importance as a “bridge” connecting other nodes. For details, refer to an introduction to network theory by Newman [54].

To capture more detailed structural information, we precompute statistics of each node’s neighbors, such as the mean and variance of neighbors’ degrees. Such statistics can be computed for semantic attributes as well (e.g., the mean age of neighbors). The neighbor statistics are shown to be useful for various analytical tasks [23, 62]. For this precomputation, we specifically use DeepGL [62] to achieve fast computation as well as to avoid producing redundant measures.

DeepGL summarizes 1-hop neighbors’ centrality/attribute values (called *base features*) with *relational functions*. For relational functions, we can specify multiple neighbor types (e.g., in-, out-, and total-neighbors) and aggregation functions (e.g., mean, variance, and maxi-

mum). After obtaining the neighbor statistics for all nodes, DeepGL prunes redundant statistics that show similar value distributions to others. The strength of pruning can be controlled with a hyperparameter of DeepGL. Moreover, DeepGL can repeatedly apply the relational functions and pruning process to summarize farther neighbors' features. For more details, refer to the work by Rossi et al. [62]. For Dataset I, as base features, we select 3 fundamental network centralities, degree, eigenvector, and betweenness, and the 14 survey attributes; then, we generate 1-hop total-neighbor statistics of the 17 attributes, resulting in 85 attributes in total after the pruning process.

3.5.2 Network Representation Learning

After selecting input and output attributes in Step 1, we first apply the Z-score normalization to each attribute. We then train an NN to predict the output from inputs, and extract representations from an NN layer (DC2: Expressivity). Although we could predict an output value directly by designing the NN for a regression task, we instead categorize output values and perform binary classification of two value ends (e.g., top and bottom 25% of attribute values). Since the classification is performed only on these ends, unrelated instances are not involved in training. If we perform regression instead, the NN tries to fit all instances. Consequently, a resulting representation may be only useful to predict values in the middle range (e.g., when fitting to the two ends is harder than the middle range). While we assume this focus on two ends is reasonable for many analyses, NNs' settings are easy to adjust based on analytical interests. Another benefit of the binary-classification design is enabling a comparison of two categorical groups (e.g., students who major in engineering and business).

By default, we use a multi-layer perceptron (MLP) consisting of five fully-connected layers (one input, three hidden, and one output layers) using the leaky rectified linear unit as an activation function. We then take the last hidden layer's activations as a learned representation. With the consideration of a balance between expressivity and interpretability, we here keep the numbers and sizes of layers sufficiently small based on the size of the input data. On the other hand, we should note that overfitting is acceptable for this step to some extent. We simplify this step's high-dimensional network representation with linear transformation in Step 3 (Sec. 3.5.3). This simplification mitigates overfitting when it occurs. The NN-based learning in Step 2 should focus on achieving an accurate alignment of the defined classes in a learned representation (i.e., high classification accuracy) rather than avoiding overfitting.

While the simple five-layer MLP is our default NN architecture, this architecture can be easily replaced with more complex ones (DC5: Extensibility). For example, when analysis needs to capture nonlinear neighbor relations in a network, we can incorporate a GNN. If learning latent vectors of links or networks is required, we can replace the precomputation of network measures, accordingly. For instance, we can extract the mean degree and network diameter for network feature learning. Then, we can apply the same procedure employing an NN.

3.5.3 Representation Simplification

We simplify the high-dimensional network representation into a 1D representation for the subsequent interpretation steps (DC3: Interpretability). Because the NN is trained for binary classification, this simplification is similar to the process NNs usually perform for their output layer: transforming the last hidden layer's activations of multiple NN nodes into a single NN node at the output layer. Therefore, we expect that although the simplified representation is 1D, it can preserve sufficient information for the prediction (DC2: Expressivity).

Our simplification employs linear transformation in contrast to nonlinear transformation. This linear transformation is the major difference from conventional NNs. A nonlinear activation function such as a sigmoid or softmax function encourages producing a value of 0 or 1 for classification. As a result, the corresponding 1D representations often consist of many values close to 0 or 1. An example of such cases is shown in Fig. 4-a. This close-to-discrete distribution makes it difficult not only to perform optimization for composite variable construction but also to observe insightful patterns from the composite variable visualization shown in Fig. 2-b.

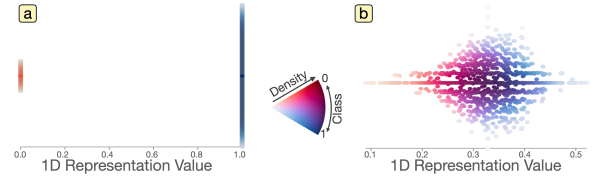


Fig. 4: 1D representations generated by alternative designs. The same dataset and visualization as Fig. 2-b1 are used (red: Class 0, blue: Class 1). (a) is made by applying a softmax activation function at the last layer of an MLP. (b) is generated by directly applying LDA to the dataset.

One way to obtain a 1D representation with linear transformation is using a linear activation function between the last hidden and output layers, as in NNs for regression tasks. As stated in Sec. 3.5.2, we, however, want to avoid directly performing regression in the NN. Instead, as a post-hoc process, we apply a DR method to the high-dimensional network representation. We specifically use LDA, which places instances of different classes as far as possible in a low-dimensional representation. This placement is achieved by maximizing the distance of each class's centroid while minimizing data variance within each class. This post-hoc process can efficiently generate a 1D representation with optimal class separation.

On the other hand, similar to NNs, LDA can easily cause overfitting when the number of instances is relatively small to the number of input features [28]. Thus, we use regularized LDA, which has a regularization mechanism to avoid overfitting [28]. The use of regularized LDA brings an additional benefit for the post-hoc approach: the regularization strength can be controlled outside of the NN training process. Although the $L1$ and $L2$ regularizations can also be used for NNs to avoid overfitting [80], the hyperparameter adjustment for these regularizations often requires many trials and errors, and becomes time-consuming by retraining NNs many times. Applying regularization inside of LDA does not require retraining of NNs and LDA is computationally efficient; thus, we can adjust the regularization strength more conveniently (DC4: Tunability).

The quality of the 1D representation can be investigated with a swarm-plot-like visualization, as shown in Fig. 2-b1. This visualization shows an instance as a dot and a 1D representation value as an x -coordinate. Similar to the swarm plot [73], y -direction is used to pile up dots with positional jitters to mitigate overplotting with a limited vertical space. The resultant area height roughly shows the frequency/density around the corresponding x -coordinate (similar to a histogram). We select this instance/point-based visualization to keep it consistent with other visualizations that use x -coordinates to represent the 1D representation values (cf. Fig. 2-b2). The color encoding is as with two-class density scatterplots'. When the 1D representation has good quality, as seen in Fig. 2-b1, two classes (Class 0: red, Class 1: blue) should have small or no overlaps. When the quality is not satisfactory, the analyst can update the NN architecture and/or the selection of input and output attributes.

In addition to the discussed architectures, we experimented with another alternative design: directly applying LDA to data to generate a 1D representation. As shown in Fig. 4-b, because this design did not exploit the strengths of NNs, the results often mixed two classes.

3.6 Understanding Representations

We describe Steps 4 and 5, which are mainly for understanding the representation obtained through Steps 1–3 (DC3: Interpretability).

3.6.1 Attribute Contribution Measurement

We extract each input attribute's contribution to the 1D representation, which is useful for two tasks. First, this attribute contribution is useful to understand each attribute's relationship to the output attribute—the interpretation from a *single attribute* level. Second, the contribution indicates attributes that should be considered for composite variables—the interpretation considering influence from *multiple attributes*.

We employ the SHAP method [46] to measure the attribute contributions. The SHAP method calculates a measure, called the SHAP value for each instance. The SHAP value is computed based on cooperative

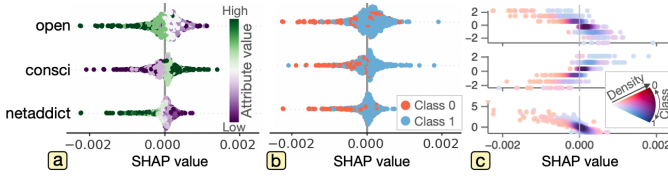


Fig. 5: Comparison of SHAP value visualizations: (a) the default plot in the SHAP package [45]; (b) the plot colored by class; and (c) our design.

game theory and shows how much a target value will be changed by adding each attribute value in a model (refer to [46] for details). We apply the SHAP method to a transferred NN model that combines the MLP trained in Step 2 and LDA trained in Step 3. In this case, the SHAP value indicates how much having a corresponding attribute value contributes to moving an instance toward a positive direction of the 1D representation. For example, when an instance’s age is 25 and its SHAP value for age is 0.1, having this age shifts the instance to a more positive side of the 1D representation by the magnitude of 0.1.

As shown in Fig. 2-a (also Fig. 5-c), we visualize SHAP values with a list of two-class density scatterplots, where each row corresponds to one attribute’s SHAP values. Our design uses x - and y -axes to depict the SHAP values and attribute values, respectively. As a summary measure of each attribute’s contribution, we use the mean absolute value of all instances’ SHAP values. We then sort the display order of the scatterplots based on this summary measure (i.e., top contributed attributes are listed from the top in order).

For example, in Fig. 2-a, we see the top 3 contributed attributes are open (openness), consci (conscientiousness), and netaddict (internet addiction). Furthermore, from the corresponding scatterplots, we can gain several insights. While larger open has a more negative impact on the 1D representation reflecting scorelevel, larger consci has a more positive impact. Also, netaddict shows clearly different patterns by Class 0 (low scorelevel) and Class 1 (high scorelevel). Larger netaddict tends to have a more negative impact for Class 0.

We tested different visual designs, as shown in Fig. 5. Fig. 5-a follows the default plot in the SHAP Python package [45], where the swarm-plot-like visualization is used. x -coordinates correspond to SHAP values, while colors inform attribute values. From this visualization, we can roughly see the relationships between these values (e.g., larger open tends to have a more negative SHAP value). But, it is infeasible to grasp patterns that differ by class. Even when juxtaposing a visualization that color-encodes class information, as shown in Fig. 5-b, we still cannot clearly see such different patterns. In contrast, our final design (Fig. 5-c) can clearly depict the relationships between SHAP and attribute values as well as different patterns by class.

3.6.2 Composite Variable Construction

The composite variable is commonly used when using a single attribute is not sufficient to understand a target phenomenon (DC2: Expressivity and DC3: Interpretability). For example, in baseball, on-base plus slugging (OPS)—the sum of two different statistics of the player’s performance, on-base percentage and slugging percentage—is used to analyze players’ contributions to team runs. This is because OPS is a simple composite variable but extremely correlates to team runs [2].

Construction algorithm. We describe the optimization algorithm designed to construct a composite variable from user-selected attributes. To explain the 1D representation with the selected attributes as much as possible, our optimization goal is to maximize a certain *measure of dependence* [61] between the 1D representation and attributes. Such measures include Pearson’s correlation, Spearman’s correlation, the mutual information. We constrain a composite variable to a linear combination of attributes to achieve a simple, intuitive interpretation as well as an efficient optimization for interactive construction.

A linear combination that achieves the highest Pearson’s correlation coefficient can be derived by multivariate linear regression. On the other hand, Spearman’s involves a non-differentiable operation to rank the 1D representation values. Due to non-differentiability, we cannot use simple regression or gradient-based solvers. Thus, we employ a gradient-free solver, specifically COBYLA (or constrained optimiza-

tion by linear approximations) [59] while using the optimized result for Pearson’s as an initial solution. Although the optimization for Pearson’s is much more efficient, Spearman’s could be more effective in some cases. This is because the 1D representation is constructed from the non-linearly transformed attributes by the NN, and the 1D representation may have a nonlinear correlation with the original input attributes. Although we currently only support Pearson’s and Spearman’s correlations, the algorithm can be easily extended for other measures of dependence (e.g., mutual information) by using COBYLA or a gradient-based solver.

Interactive use. From the view in Fig. 2-a, an analyst can select attributes and a measure of dependence, and then generate a composite variable by clicking “Construct New Composite Variable” located at the bottom. The selected attributes are highlighted with gray backgrounds. Then, a two-class density scatterplot (Fig. 2-b2) visualizes the relationships between the 1D representation (x -axis) and the constructed composite variable (y -axis). Also, multiple composite variables can be created to compare their expressivity and interpretability (DC4: Tunability). A newly constructed composite variable’s visualization is appended to a list of the scatterplots in a scrollable view. Each scatterplot can be discarded by clicking a “ \times ” mark at the top right.

In essence, through this composite variable construction process, analysts can utilize their domain knowledge to review the simplified representation. From the attributes ranked by SHAP values, the analyst can judge attributes they should consider. Then, with the help of the above optimization algorithm, the analyst can interactively examine and fine-tune the composite variables to gain insights.

Analysis examples. For Dataset I, we compute Spearman’s correlation coefficient between each of the top 5 contributed attributes and the 1D representation. The coefficients are open: -0.147, consci: 0.237, netaddict: 0.134, min_happy (the minimum of friends’ happiness levels): 0.093, and extra (extraversion): 0.026. As shown in Fig. 2-b2, using all these attributes, we can generate a composite variable that has a better correlation coefficient, 0.300, than any single attribute. This coefficient is in a moderate correlation group based on Dancey and Reidy’s categorization [17]. We follow Dancey and Reidy’s categorization in the rest of the paper when describing correlation strengths.

Since all attributes are normalized, each attribute’s weight in the composite variable shows a contribution level to the composite variable (open: -0.4, consci: +0.7, netaddict: -0.3, min_happy: +0.3, extra: +0.3). consci contributes most, as expected from its higher Spearman’s correlation (0.237) than others. In contrast, extra is assigned a relatively large weight (+0.3) in spite of its extremely small correlation (0.026) as a single attribute. The importance of extra can be confirmed by excluding extra from the composite variable construction. When extra is extruded, the composite variable’s correlation coefficient decreases from 0.300 to 0.289. From further interactive investigations on how the inclusion of extra improves each other attribute’s correlation, we observe that open has a much larger improvement (from 0.147 to 0.170) than others (e.g., consci has no improvement). We can infer that, by including open and extra with different signs (-0.4 and 0.3), the composite variable captures the subtle difference between these two personalities. Then, scorelevel shows higher dependence on this derived difference than either open or extra. This type of insight cannot be derived if only investigating a single attribute relationship to the 1D representation. Also, this example demonstrates the effectiveness of the SHAP-based recommendation in contrast to relying only on each attribute’s correlation coefficient.

We should emphasize that while we want to make a composite variable correlated to the 1D representation to some extent (e.g., Spearman’s ≥ 0.2 , weakly correlated), we do not have to see extremely correlated results (e.g., Spearman’s ≥ 0.7 , strongly correlated). If a strong correlation can be found with a linear combination of a few attributes, the use of NNs becomes unnecessary. In such a case, linear learning methods such as LDA should be sufficient for the prediction. Our focus is taking a further step from the single-attribute-based interpretation using the SHAP or other methods [39, 46, 53]. Our approach considers the influence of multiple attributes. Such an influence can be analyzed via the signed weights in a composite variable and the

interactive adjustment of the composite variable. The correlations to each composite variable should be considered as an indicator of how much of the 1D representation is explained with the composite variable.

3.7 Interactive Visual Interface

All visualizations in the UI are fully linked and share the same or similar color encodings (e.g., red represents Class 0). Lasso selection can be performed in Fig. 2-a, b, c. The selected instances from Classes 0 and 1 will be highlighted in yellow (e.g., Fig. 7-c). With this linking, analysts can investigate specific patterns, such as outliers and subgroups. We further provide visualizations of structural and semantic information to supplement the interpretation of the results.

Structural information. Fig. 2-c shows network layouts as the structural information. Only in this view, we visualize all instances even including those not belonging to the two ends (i.e., Classes 0 and 1). This is because the precomputed network measures (e.g., degree) used for NRL are computed using links among all instances. And, we need to review the entire network to locate patterns related to the structural information. We apply scalable force-directed placement (SFDP) [32] and then use red, blue, and gray colors to represent Class 0, Class 1, and other instances, respectively.

Attribute information. We visualize the distribution of each attribute as a double-bar histogram. By default, as shown in Fig. 2-d, the UI shows the distribution for each class. When the lasso selection is performed, we show the distributions of selected and non-selected instances (e.g., Fig. 6-b1 and b2). Because we have limited screen space, we order histograms based on the two groups' distribution differences measured by the Kolmogorov-Smirnov (KS) statistic.

Implementation. The UI is developed as a web application. For the back end, Python is used to perform Step 1 with DeepGL, Step 2 with MLPs, Step 3 with regularized LDA, Step 4 with the SHAP method, Step 5 with multivariate regression and the COBYLA, and Step 6 with the two-class density scatterplot, SFDP, and KS statistic. The implementation of these algorithms utilizes various libraries, such as deepgl [24], PyTorch [56] (for MLPs), ulca [22] (for regularized LDA), SHAP [45], Scikit-learn [57] (for multivariate regression), NumPy/SciPy [70] (for the COBYLA, KS statistic, and Gaussian kernel density estimation), graph-tool [58] (for SFDP), seaborn [74] (for the swarm-like visualization), and ColorAide [52] (for color generation). The front-end UI is implemented with HTML5, JavaScript, and D3 [6]. WebSocket is used for communication between the front- and back-end modules.

4 CASE STUDIES

We demonstrate the effectiveness of our workflow and interactive visualizations with three case studies using the two datasets. For the first two case studies on Dataset I, we show analyses on network nodes. In the third case, we analyze the egocentric networks of Dataset II.

4.1 Study 1: Associations with Score Levels

We present a complete version of the analysis we have performed in Sec. 3.5 and Sec. 3.6. Our analysis target is the identification of attributes that are highly related to college students' `scorelevel`. We classify the bottom and top `scorelevel` groups with the five-layer MLP using 128, 64, and 64 NN nodes for hidden layers. 138 and 648 students are categorized into the bottom group (Class 0, red color) and top group (Class 1, blue color), respectively. The prediction results show 1.0 accuracy for Step 2 but 0.98 for Step 3 (refer to Sec. 3.5.2 for the reason why we accept such high accuracies).

After completing Steps 1–3, we first confirm that the extracted 1D representation provides a reasonable separation between the two classes, as shown in Fig. 2-b1,. Also, the distribution of instances/students shows a sufficient variety in their coordinates. Thus, we expect that the 1D representation is not extremely overfitted for this classification.

We then review attributes' associations with the 1D representation from the view in Fig. 2-a. Based on the ranked order of the attributes, contributing attributes to the score level differences are highly related to many of the Big Five personality traits: `open` (openness), `consci` (conscientiousness), `extra` (extraversion), `neuro` (neuroticism), and `agree` (agreeableness). Other highly ranked attributes include `netaddict` (internet addiction level) and `min_happy` (the minimum of the friends'

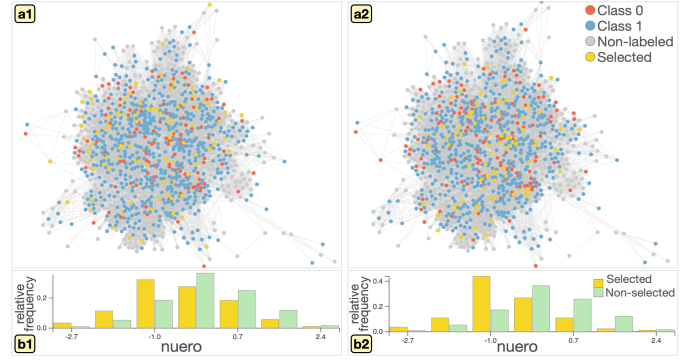


Fig. 6: Study 1: Networks after selecting students with (a1) high ($-0.9 \text{ open} + 0.4 \text{ extra}$) and (a2) high extra; distributions of `neuro` (b1, b2) corresponding to the selections of (a1, a2).

happiness levels). On the other hand, most network centralities are not ranked high. As we examined in Sec. 3.6.1, the top 5 attributes have clear positive or negative trends with the SHAP values (e.g., higher `open` value tends to have a more negative SHAP value).

Next, we construct a composite variable with the top 5 attributes while using Spearman's as a measure of dependence. Fig. 2-b2 visualizes the result. The composite variable is expressed as: $y = -0.4 \text{ open} + 0.7 \text{ consci} - 0.3 \text{ netaddict} + 0.3 \text{ min_happy} + 0.3 \text{ extra}$. Each weight's sign agrees with the corresponding attribute's positive or negative influence on the 1D representation, which is observed in Fig. 2-a. Based on the magnitudes, we can see `consci` contributes most to the 1D representation. Also, as discussed in Sec. 3.6.2, we observe that `open` and `extra`—personalities that might have some overlapped aspect—likely derive a new meaningful attribute by having opposite signs with each other. When a composite variable is constructed with these two attributes, the resultant variable, $-0.9 \text{ open} + 0.4 \text{ extra}$, shows a 0.17 correlation coefficient. Thus, having both openness and introversion tends to have clear negative impacts on their score levels.

We want to investigate another question raised during the above analysis: why network centralities were not listed as highly contributed attributes even though the composite variable, $-0.9 \text{ open} + 0.4 \text{ extra}$, shows a clear contribution to the 1D representation. Openness and extraversion could be related to network centralities such as node degree (e.g., extrovert students are likely to have more friends). To examine the relationships to network structure, we highlight students with low ($-0.9 \text{ open} + 0.4 \text{ extra}$) in the network layout visualization, as shown in Fig. 6-a1. While we see several selected students (colored yellow) are located on the outskirts of the network (i.e., fewer connections to others), we cannot find any clear structural pattern. When selecting students with high `extra` (Fig. 6-a2), we cannot see a clear pattern either. Thus, we can expect that openness and extraversion in real life were difficult to capture only from the connections on Facebook.

We further see the UI suggests `neuro` shows strongly different distributions between the selected and non-selected students. From the distributions of `neuro` shown in Fig. 6-b1 and b2, the students with high ($-0.9 \text{ open} + 0.4 \text{ extra}$) or high `extra` tend to have lower `neuro` than others. Therefore, `neuro` is also interrelated to `open` and `extra`. However, based on Fig. 2-a, `neuro` has a smaller influence on the score level and does not show consistent positive or negative influences among students. In fact, the inclusion of `neuro` into the composite variable of the top 5 attributes does not improve the correlation coefficient.

The above observations derive several reasonable insights: The student's conscientiousness is highly related to their score level; internet addiction has a negative association with the score, especially, for those who had bad scores (refer to Sec. 3.6.1); if all friends have sufficient happiness, the score tends to be higher, and vice versa; and the openness and extraversion show a clear combinational effect and a high openness with a low extraversion has a more negative relationship to the score.

4.2 Study 2: Differences in Academic Units

From Dataset I, we review whether students from different majors have different structural and semantic characteristics. To per-

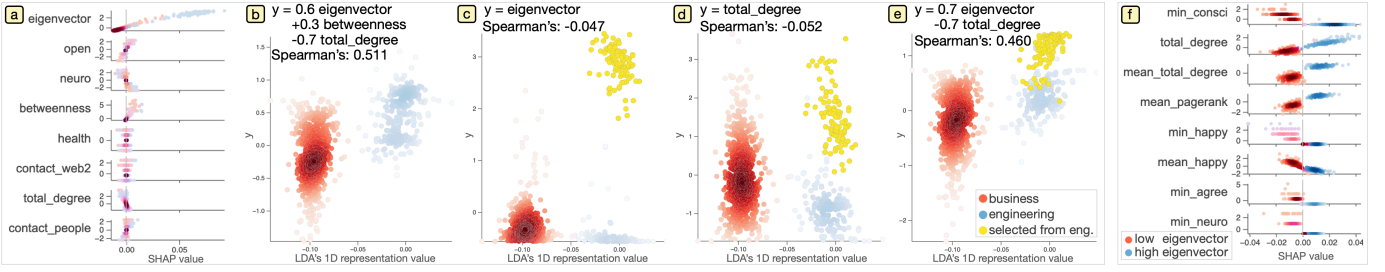


Fig. 7: Study 2: The comparison of groups. (a-e) business and engineering students; (f) engineering students with high and low eigenvector.

form this comparison, we select each pair of all possible different majors (agricultural, business, engineering, humanities, physical sciences, and social sciences). We reviewed all pairs, but here we show one representative analysis: the comparison of business (Class 0, red, 801 students) and engineering (Class 1, blue, 287 students). We use the same 85 attributes and MLP as Study 1 and perform classification of business and engineering. The prediction results show 1.0 accuracy for both Steps 2–3.

Fig. 7-a shows the top 8 contributed attributes to the differences between business and engineering. Unlike Study 1, this list of the top 8 includes network centralities, eigenvector, betweenness, and total_degree. To see the associations between these centralities and the 1D representation, we generate a composite variable with these three centralities, as shown in Fig. 7-b. The resultant composite variable shows a moderate correlation (Spearman’s: 0.511). Also, we can see large weights with opposite signs for eigenvector and total_degree (+0.6 and −0.7). Unlike degree, eigenvector centrality considers the importance of links (discussed in Sec. 3.5.1). Taking a subtraction of degree from eigenvector centrality can emphasize this unique characteristic of eigenvector centrality.

As Fig. 7-a depicts a clear positive influence of high eigenvector, we visualize the relationships between eigenvector and the 1D representation. From the result shown in Fig. 7-c, we first notice that eigenvector itself has a very small correlation coefficient (−0.047). At the same time, there are two clear subgroups in a group of engineering as we highlight one group in yellow. On the other hand, as shown in Fig. 7-d, a similar but more moderate separation can be seen in total_degree. We then construct a new composite variable with only eigenvector and total_degree. The result shown in Fig. 7-e informs a clear correlation of this new composite variable to the 1D representation (+0.460). From the visualizations in Fig. 7-c, d, and e, we now grasp how this informative composite variable for the difference of business and engineering is generated from the two centralities. This result emphasizes the importance of interpretation using a mix of multiple attributes.

We are further interested in understanding the difference between low and high eigenvector groups in engineering students. To perform this analysis, we select these two groups as a classification target. Fig. 7-f shows the derived top 8 contributing attributes, where red and blue colors are now used for low and high eigenvector groups. Most attributes show a clear separation between the groups. Also, many of them are related to the student’s personality or mentalities, such as consci, happy, and agree. Meanwhile, the listed attributes in Fig. 7-f tend to correspond with the minimum values of their friends’, as indicated with the prefix, “min_”. As the high eigenvector group tends to have high total_degree (see Fig. 7-d), the students in the high eigenvector group are likely to have many friends, resulting in a higher chance to have at least one friend with low values for these attributes. Therefore, we consider that this result is caused by inappropriate fittings specific to these two groups. As taking the minimum of 1-hop neighbor statistics was problematic, we should adjust the feature extraction parameters to examine these groups’ differences.

From this study, we observe the difference between business and engineering students in the composite variable constructed with the network centralities. As the composite variable emphasizes the difference between the eigenvector and total degree centralities, engineering students’ connections tend to be more particular to in-

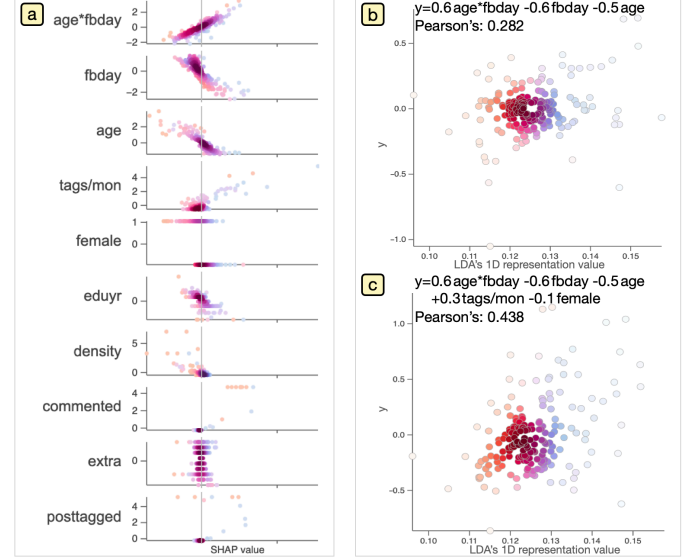


Fig. 8: Study 3: (a) The top contributing attributes and composite variables constructed with (b) the top 3 and (c) top 5 attributes.

fluent students in Facebook. Also, we demonstrate the case of identifying potential inappropriate overfitting from the visualized results.

4.3 Study 3: Factors Promoting New Connections

From Dataset II containing 345 egocentric networks of adults, we review contributing factors to promoting their indirect contacts (i.e., 2-hop neighbors) to direct contacts (i.e., 1-hop neighbors). For each network, we first compute the ratio of the number of indirect contacts transformed into direct contacts during the study period. We call this ratio the transformation rate and denote it as r . We then group respondents (i.e., ego nodes) with conditions of $r=0$ (i.e., no transformation) as Class 0 and $r \geq 0.2$ (i.e., high transformation rate) as Class 1. Classes 0 and 1 consist of 56 and 136 respondents, respectively. We then perform the classification of these classes, resulting in accuracies of 1.0 and 0.82 for Steps 2 and 3.

Fig. 8-a shows the top 10 contributed attributes to the 1D representation. We see several clear trends between attributes’ values and the SHAP values. For example, age*fbdays shows an increasing trend (i.e., larger age*fbdays has a more positive impact on the transformation). age*fbdays is the predefined composite variable by the existing study [41]. This attribute is made by multiplying the ego’s age and total days of Facebook use, fbdays. Due to this definition of age*fbdays, all top 3 contributed attributes, age*fbdays, fbdays, age, are likely to interrelate with each other. Then, we construct a composite variable with these attributes. As shown in Fig. 8-b, the constructed composite variable, $0.6 \text{ age*fbdays} - 0.6 \text{ fbdays} - 0.5 \text{ age}$, presents a weak correlation (Pearson’s: 0.282). By investigating three attributes individually, we observe that they show a much weaker correlation to the 1D representation—age*fbdays: 0.064, fbdays: 0.052, age: 0.123. Thus, the composite variable seems to find more meaningful information by disentangling complex relationships among the three attributes. We further construct a new composite variable by adding other highly ranked attributes, tags/mon (the average times of being tagged per month) and

female (whether ego’s gender is female or not). As shown in Fig. 8-c, the new composite variable has a significantly stronger correlation than the previous one (0.438 vs. 0.282).

For verification, we compare our findings with the existing study [41]. The existing study employed a mixed-effect model to capture attributes’ contributions to the transformation of indirect contacts. The top 5 contributed attributes suggested by their model are female, extra, comments/mon (the average number of comments made per month), fbday, and age*fbday. First of all, three attributes, age*fbday, fbday, and female, are seen in both their results and ours. Also, tags/mon and comments/mon should have semantic similarities with each other based on their meanings. In fact, by replacing tags/mon with comments/mon, we obtain the composite variable with 0.382 Pearson’s correlation coefficient, which is considerably close to the original (Pearson’s: 0.438). These observations indicate that our NN-based model successfully captured similar information to the mixed-effect model. The unique strength of our approach is in its ability to convey inter-relationships of attributes with their weights in the composite variable. While the existing work [41] crafted age*fbday, our study suggests $(0.6 \text{ age*fbday} - 0.6 \text{ fbday} - 0.5 \text{ age})$ or a more simplified version, $(\text{age*fbday} - \text{fbday} - \text{age})$, as a potential composite variable that better capture the influence on the transformation than age*fbday.

5 EXPERT FEEDBACK

To further validate our workflow’s usability, we conducted an informal interview with experts in social network studies. The first expert (E1) is a distinguished researcher in an institute of sociology who collected Datasets I and II and also conducted research on these datasets with different focuses from ours. The second expert (E2) is an assistant professor in a department of sociology who formulated the guidelines for collecting the datasets. The other three experts are researchers in institutes of sociology (E3) and statistical science (E4, E5) who also studied the same datasets. The interview was conducted through a video conference setup, where the preliminary versions of the three case studies were presented.

All the experts agreed that our workflow can support a wide range of their analysis targets as well as derive insights with more intuitive interpretations when compared to their current approach. For example, E1 commented, “The results [seen in the composite variables] are much easier to understand and intuitive than the outputs from the statistical models used in our previous research.” All of them showed strong interest in insights that can be derived from the signed weights in composite variables. On the other hand, E1 noted a potential limitation of the datasets and analyses: “The distribution of the respondents might affect the results related to the internet addiction because the students who granted the use of their data tended to be more addicted to the internet usage than others.” E2 suggested better input attributes for the analyses, and we improved our case studies, accordingly.

There are several discussions on our workflow usage and design. E3 asked, “What if there are attributes with a dominant influence on the result? What if the 1D representation does not have clear separation?” For the former, the visualization shown in Fig. 2-a can be used to identify dominant attributes and exclude them from inputs if such attributes exist. Similarly, for the latter case, the visualization shown in Fig. 2-b1 is useful to review the quality of the separation. Then, based on the quality, analysts can take actions, such as adding more input attributes, reducing the ranges of the two ends of the output attribute, and improving the NN model. E4 raised a question on our post-hoc simplification of network representations: “Why not only use a neural network by designing the last layer with a linear activation function, instead of using LDA?” Our answer is given in Sec. 3.5.3. E5 asked, “Why not use other centralities but these three?” We selected degree, eigenvector, and betweenness centralities as a set of the most fundamental measures of structural characteristics. Our workflow is flexible to employ any other centralities based on analysts’ interests.

6 DISCUSSION

Through the case studies and the expert interview, we discussed the effectiveness of our workflow and interactive visualizations. Besides

these evaluations, to allow readers to test our workflow and UI, we provide related source code as well as processed data [1] from a publicly available dataset of faculty networks [72]. Here, we provide additional discussions on our designs.

Applicability to various data types. We have designed our workflow for multivariate networks. As multivariate networks have both high-dimensional and relational characteristics, by their nature, the workflow is even applicable to high-dimensional data and univariate network data. For example, we can analyze high-dimensional data by skipping the extraction of network centrality-related attributes and the visualization of networks. In addition, our workflow design can potentially adapt to advanced models of networks such as those containing meta-nodes and hyperedges. For example, as long as meta-nodes have the same set of node attributes as simple nodes in a network, we can still apply our workflow as is. Our workflow precomputes node- and link-related features before the training utilizing NNs; thus, we can deal with hyperedges during this preprocessing step (e.g., including hyperedges when applying relational functions in DeepGL).

Other potential algorithm designs. While we employ the NNs, DR, and composite variable construction to support our analysis target, there are other potential designs. One common way to understand the associations among a target and other attributes is applying a decision tree (DT) [7, 43]. When compared with a DT-based analysis, our design provides two main strengths in the interpretation step: simplicity and informativity. A DT provides a set of attribute ranges that is useful to classify a target attribute. However, the number of ranges would be easily overwhelming when analyzing networks with many attributes. Also, from the DT results, it is difficult to numerically assess the influences from multiple attributes, such as those seen in the composite variables we have constructed for the case studies.

Another possible design is enabling the construction of more complicated composite variables, such as those with multiplications and logarithms of attributes. Although this would be more effective to analyze complex relationships among attributes (e.g., age*fbday in Sec. 4.3), this construction requires much more complicated optimizations than ours. One potential way to perform such advanced constructions while avoiding excessive computation is incorporating analysts’ knowledge more actively (e.g., predetermining a part of a composite variable). We plan to investigate this direction in future research.

Usability of two-class density scatterplots. We developed two-class density scatterplots to depict various patterns (e.g., distributions of class instances, trends, clusters, and outliers) in a single visualization. The use of this scatterplot is not limited to the targeted analyses in this work. As binary classifications or group comparisons are frequently performed for machine learning and visual analytics, we believe two-class density scatterplots can contribute to these fields. As future research, we plan to conduct a comprehensive user study to evaluate the effectiveness of our scatterplot design as well as to identify its shortcomings for further improvements. There is one clear limitation: allowing visualization of only two classes. One potential way to support three or more classes is taking similar approaches to the multiclass geographical maps by Jo et al. [34]. For example, we can first partition a 2D space based on the changes in the distribution of class instances and then display the distribution in each partitioned region with a bar-chart glyph. We expect that this design can deal with several classes (e.g., five classes); however, this partition-based approach would not be suitable to reveal outliers and clusters. Thus, we would like to investigate an extension to three or more classes in the future.

7 CONCLUSION

We have introduced a new visual analytics workflow designed to help find associations from complex multivariate networks. The workflow integrates neural-network-based representation learning, composite variable construction, and interactive visualizations. Benefiting from these components, the workflow generates expressive as well as interpretable analytical results. The design of workflow is also suited for analyzing other simpler types of data, such as a univariate network and high-dimensional data. Thus, our work potentially contributes to a wide range of applications that involve analyses of large, complex data.

ACKNOWLEDGMENTS

This work has been supported in part by the National Institute of Health through grants 1R01CA270454-01 and 1R01CA273058-01 and by the Knut and Alice Wallenberg Foundation through Grant KAW 2019.0024.

REFERENCES

- [1] The supplementary materials: Source code, data, and a demonstration video. <https://github.com/hylu1994/Network-CV>.
- [2] J. Albert. Sabermetrics: The past, the present, and the future. In J. A. Gallian, ed., *Mathematics and Sports*, p. 3–14. Mathematical Association of America, 2010. doi: 10.5948/UPO9781614442004.002
- [3] M. Atzmueller, S. Günnemann, and A. Zimmermann. Mining communities and their descriptions on attributed graphs: A survey. *Data Min Knowl Disc*, 35(3):661–687, 2021. doi: 10.1007/s10618-021-00741-z
- [4] B. Bach, C. Shi, N. Heulot, T. Madhyastha, T. Grabowski, and P. Dragicevic. Time Curves: Folding time to visualize patterns of temporal evolution in data. *IEEE Trans Vis Comput Graph*, 22(1):559–568, 2016. doi: 10.1109/TVCG.2015.2467851
- [5] F. Beck, M. Burch, S. Diehl, and D. Weiskopf. A taxonomy and survey of dynamic graph visualization. *Comput Graph Forum*, 36(1):133–159, 2017. doi: 10.1111/cgf.12791
- [6] M. Bostock, V. Ogievetsky, and J. Heer. D³ data-driven documents. *IEEE Trans Vis Comput Graph*, 17(12):2301–2309, 2011. doi: 10.1109/TVCG.2011.185
- [7] J. E. Brand, J. Xu, B. Koch, and P. Geraldo. Uncovering sociological effect heterogeneity using tree-based machine learning. *Sociol Methodol*, 51(2):189–223, 2021. doi: 10.1177/0081175021993503
- [8] M. Cavallo and Ç. Demiralp. A visual interaction framework for dimensionality reduction based data exploration. In *Proc. CHI*, pp. 1–13, 2018. doi: 10.1145/3173574.3174209
- [9] M.-y. Chang and Y.-c. Fu. Social media and network boundaries among college students: Reconstructing companions, conversations, and contact circles. *Taiwanese Sociology*, 37:1–46, 2019. Written in Chinese. doi: 10.6676/TS.201906_(37).02
- [10] A. Chatzimparmpas, R. M. Martins, I. Jusufi, K. Kucher, F. Rossi, and A. Kerren. The state of the art in enhancing trust in machine learning models with the use of visualizations. *Comput Graph Forum*, 39(3):713–756, 2020. doi: 10.1111/cgf.14034
- [11] A. Chatzimparmpas, R. M. Martins, and A. Kerren. t-viSNE: Interactive assessment and interpretation of t-SNE projections. *IEEE Trans Vis Comput Graph*, 26(8):2696–2714, 2020. doi: 10.1109/tvcg.2020.2986996
- [12] Q. Chen, N. Chen, W. Shuai, G. Wu, Z. Xu, H. Tong, and N. Cao. CalliopeNet: Automatic generation of graph data facts via annotated node-link diagrams. *IEEE Trans Vis Comput Graph*, 2023 (forthcoming). doi: 10.48550/arXiv.2308.06441
- [13] R. Chetty, M. O. Jackson, T. Kuchler, J. Stroebe, N. Hendren, et al. Social capital I: Measurement and associations with economic mobility. *Nature*, 608:108–121, 2022. doi: 10.3386/w30313
- [14] T. Crnovrsanin, C. W. Muelder, R. Faris, D. Felmlee, and K.-L. Ma. Visualization techniques for categorical analysis of social networks with multiple edge sets. *Soc Networks*, 37:56–64, 2014. doi: 10.1016/j.socnet.2013.12.002
- [15] J. P. Cunningham and Z. Ghahramani. Linear dimensionality reduction: Survey, insights, and generalizations. *J. Mach. Learn. Res.*, 16(1):2859–2900, 2015. doi: 10.48550/arXiv.1406.0873
- [16] J. P. Cunningham and B. M. Yu. Dimensionality reduction for large-scale neural recordings. *Nat Neurosci*, 17(11):1500–1509, 2014. doi: 10.1038/nn.3776
- [17] C. P. Dancy and J. Reidy. *Statistics without maths for psychology*. Pearson London, 2017.
- [18] R. Faust, D. Glickenstein, and C. Scheidegger. DimReader: Axis lines that explain non-linear projections. *IEEE Trans Vis Comput Graph*, 25(1):481–490, 2018. doi: 10.1109/tvcg.2018.2865194
- [19] M. Freire, C. Plaisant, B. Shneiderman, and J. Golbeck. ManyNets: An interface for multiple network analysis and visualization. In *Proc. CHI*, pp. 213–222, 2010. doi: 10.1145/1753326.1753358
- [20] T. Fujiwara, J.-K. Chou, A. M. McCullough, C. Ranganath, and K.-L. Ma. A visual analytics system for brain functional connectivity comparison across individuals, groups, and time points. In *Proc. PacificVis*, pp. 250–259, 2017. doi: 10.1109/pacificvis.2017.8031601
- [21] T. Fujiwara, O.-H. Kwon, and K.-L. Ma. Supporting analysis of dimensionality reduction results with contrastive learning. *IEEE Trans Vis Comput Graph*, 26(1):45–55, 2020. doi: 10.1109/tvcg.2019.2934251
- [22] T. Fujiwara, X. Wei, J. Zhao, and K.-L. Ma. Interactive dimensionality reduction for comparative analysis. *IEEE Trans Vis Comput Graph*, 28(1):758–768, 2022. doi: 10.1109/tvcg.2021.3114807
- [23] T. Fujiwara, J. Zhao, F. Chen, and K.-L. Ma. A visual analytics framework for contrastive network analysis. In *Proc. VAST*, pp. 48–59, 2020. doi: 10.1109/vast50239.2020.00010
- [24] T. Fujiwara, J. Zhao, F. Chen, Y. Yu, and K.-L. Ma. Network comparison with interpretable contrastive network representation learning. *J Data Sci Stat Vis*, 2(5), 2022. doi: 10.52933/jdssv.v2i5.56
- [25] M. Gleicher. Explainers: Expert explorations with crafted projections. *IEEE Trans Vis Comput Graph*, 19(12):2042–2051, 2013. doi: 10.1109/tvcg.2013.157
- [26] R. Gove. Gragnostics: Fast, interpretable features for comparing graphs. In *Proc. IV*, pp. 201–209, 2019. doi: 10.1109/iv.2019.00042
- [27] A. Grover and J. Leskovec. node2vec: Scalable feature learning for networks. In *Proc. KDD*, pp. 855–864, 2016. doi: 10.1145/2939672.2939754
- [28] Y. Guo, T. Hastie, and R. Tibshirani. Regularized linear discriminant analysis and its application in microarrays. *Biostat*, 8(1):86–100, 2007. doi: 10.1093/biostatistics/kxj035
- [29] W. Hamilton, Z. Ying, and J. Leskovec. Inductive representation learning on large graphs. In *Proc. NIPS*, pp. 1024–1034, 2017. doi: 10.48550/arXiv.1706.02216
- [30] R. Hamon, H. Junklewitz, and I. Sanchez. Robustness and explainability of artificial intelligence. Technical Report KJ-NA-30040-EN-N (online), Publications Office of the European Union, 2020. doi: 10.2760/57493
- [31] M. Harrigan, D. Archambault, P. Cunningham, and N. Hurley. EgoNav: Exploring networks through egocentric spatializations. In *Proc. AVI*, pp. 563–570, 2012. doi: 10.1145/2254556.2254661
- [32] Y. Hu. Efficient, high-quality force-directed graph drawing. *Math J*, 10(1):37–71, 2005.
- [33] Z. Huang, D. Witschard, K. Kucher, and A. Kerren. VA + embeddings STAR: A state-of-the-art report on the use of embeddings in visual analytics. *Comput Graph Forum*, 42(3):539–571, 2023. doi: 10.1111/cgf.14859
- [34] J. Jo, F. Vernier, P. Dragicevic, and J.-D. Fekete. A declarative rendering model for multiclass density maps. *IEEE Trans Vis Comput Graph*, 25(1):470–480, 2018. doi: 10.1109/tvcg.2018.2865141
- [35] P. Joia, F. Petronetto, and L. G. Nonato. Uncovering representative groups in multidimensional projections. *Comput Graph Forum*, 34(3):281–290, 2015. doi: 10.1111/cgf.12640
- [36] A. Kerren, H. C. Purchase, and M. O. Ward, eds. *Multivariate Network Visualization*, vol. 8380 of *Lect Notes Comput Sci*. Springer, 2014. doi: 10.1007/978-3-319-06793-3
- [37] T. N. Kipf and M. Welling. Semi-supervised classification with graph convolutional networks. In *Proc. ICLR*, pp. 1–10, 2017. doi: 10.48550/arXiv.1609.02907
- [38] J. Knittel, A. Lalama, S. Koch, and T. Ertl. Visual neural decomposition to explain multivariate data sets. *IEEE Trans Vis Comput Graph*, 27(2):1374–1384, 2020. doi: 10.1109/tvcg.2020.3030420
- [39] B. C. Kwon, B. Eysenbach, J. Verma, K. Ng, C. De Filippi, W. F. Stewart, and A. Perer. Clustervision: Visual supervision of unsupervised clustering. *IEEE Trans Vis Comput Graph*, 24(1):142–151, 2018. doi: 10.1109/tvcg.2017.2745085
- [40] O.-H. Kwon, T. Crnovrsanin, and K.-L. Ma. What would a graph look like in this layout? A machine learning approach to large graph visualization. *IEEE Trans Vis Comput Graph*, 24(1):478–488, 2018. doi: 10.1109/tvcg.2017.2743858
- [41] H.-W. Lee, M.-Y. Chang, W.-Y. Chou, J.-S. Hwang, and Y.-C. Fu. From indirect to direct contacts on Facebook: A big-data approach to the making of triadic network closure. *Can Rev Sociol*, 59(2):207–227, 2022. doi: 10.1111/cars.12375
- [42] S. Lespinats and M. Aupetit. CheckViz: Sanity check and topological clues for linear and non-linear mappings. *Comput Graph Forum*, 30(1):113–125, 2011. doi: 10.1111/j.1467-8659.2010.01835.x
- [43] Y. Li, E. Musabandesu, T. Fujiwara, F. J. Loge, and K.-L. Ma. A visual analytics system for water distribution system optimization. In *Proc. VIS*, pp. 126–130, 2021. doi: 10.1109/vis49827.2021.9623272
- [44] M. Lu, S. Wang, J. Lanir, N. Fish, Y. Yue, D. Cohen-Or, and H. Huang. Winglets: Visualizing association with uncertainty in multi-class scatter-

- plots. *IEEE Trans Vis Comput Graph*, 26(1):770–779, 2020. doi: 10.1109/tvcg.2019.2934811
- [45] S. M. Lundberg. SHAP (SHapley Additive exPlanations). <https://github.com/slundberg/shap>, 2018. Accessed: 2022-12-28.
- [46] S. M. Lundberg and S.-I. Lee. A unified approach to interpreting model predictions. In *Proc. NIPS*, vol. 30, 2017. doi: 10.48550/arXiv.1705.07874
- [47] D. Malerba, F. Esposito, and G. Semeraro. A further comparison of simplification methods for decision-tree induction. In D. Fisher and H.-J. Lenz, eds., *Learning from Data: Artificial Intelligence and Statistics V*, pp. 365–374. Springer New York, 1996. doi: 10.1007/978-1-4612-2404-4_35
- [48] R. M. Martins, G. F. Andery, H. Heberle, F. V. Paulovich, A. de Andrade Lopes, H. Pedrini, and R. Minghim. Multidimensional projections for visual analysis of social networks. *J Comput Sci Technol*, 27(4):791–810, 2012. doi: 10.1007/s11390-012-1265-5
- [49] R. M. Martins, J. F. Kruiger, R. Minghim, A. C. Telea, and A. Kerren. MVN-Reduce: Dimensionality reduction for the visual analysis of multivariate networks. In *Proc. EuroVis*, pp. 13–17, 2017. doi: 10.2312/eurovisshort.20171126
- [50] A. Mayorga and M. Gleicher. Splatterplots: Overcoming overdraw in scatter plots. *IEEE Trans Vis Comput Graph*, 19(9):1526–1538, 2013. doi: 10.1109/tvcg.2013.65
- [51] F. McGee, M. Ghoniem, G. Melançon, B. Otjacques, and B. Pinaud. The state of the art in multilayer network visualization. *Comput Graph Forum*, 38(6):125–149, 2019. doi: 10.1111/cgf.13610
- [52] I. Muse. ColorAide. <https://facelessuser.github.io/coloraide/>, 2020. Accessed: 2022-12-29.
- [53] M. P. Neto and F. V. Paulovich. Multivariate data explanation by jumping emerging patterns visualization. *arXiv:2106.11112*, 2021. doi: 10.48550/arXiv.2106.11112
- [54] M. Newman. *Networks*. Oxford University Press, 2018.
- [55] C. Nobre, M. Meyer, M. Streit, and A. Lex. The state of the art in visualizing multivariate networks. *Comput Graph Forum*, 38(3):807–832, 2019. doi: 10.1111/cgf.13728
- [56] A. Paszke, S. Gross, F. Massa, A. Lerer, J. Bradbury, et al. PyTorch: An imperative style, high-performance deep learning library. In *Proc. NeurIPS*, pp. 8024–8035, 2019. doi: 10.48550/arXiv.1912.01703
- [57] F. Pedregosa, G. Varoquaux, A. Gramfort, V. Michel, B. Thirion, et al. Scikit-learn: Machine learning in Python. *J Mach Learn Res*, 12:2825–2830, 2011. doi: 10.48550/arXiv.1201.0490
- [58] T. P. Peixoto. The graph-tool python library. *figshare*, 2014. http://figshare.com/articles/graph_tool/1164194.
- [59] M. J. Powell. Direct search algorithms for optimization calculations. *Acta Numerica*, 7:287–336, 1998. doi: 10.1017/s0962492900002841
- [60] N. Pržulj. Biological network comparison using graphlet degree distribution. *Bioinformatics*, 23(2):e177–e183, 2007. doi: 10.1093/bioinformatics/btq091
- [61] Y. A. Reshef, D. N. Reshef, H. K. Finucane, P. C. Sabeti, and M. Mitzenmacher. Measuring dependence powerfully and equitably. *J Mach Learn Res*, 17(1):7406–7468, 2016. doi: 10.48550/arXiv.1505.02213
- [62] R. A. Rossi, R. Zhou, and N. Ahmed. Deep inductive graph representation learning. *IEEE Trans Knowl Data Eng*, 32(3):438–452, 2018. doi: 10.1109/TKDE.2018.2878247
- [63] A. Sarikaya and M. Gleicher. Scatterplots: Tasks, data, and designs. *IEEE Trans Vis Comput Graph*, 24(1):402–412, 2018. doi: 10.1109/tvcg.2017.2744184
- [64] H. Song, Z. Dai, P. Xu, and L. Ren. Interactive visual pattern search on graph data via graph representation learning. *IEEE Trans Vis Comput Graph*, 28(1):335–345, 2022. doi: 10.1109/tvcg.2021.3114857
- [65] M.-K. Song, F.-C. Lin, S. E. Ward, and J. P. Fine. Composite variables: When and how. *Nurs Res*, 62(1):45, 2013. doi: 10.1097/nnr.0b013e3182741948
- [66] The Matplotlib development team. Choosing colormaps in matplotlib. <https://matplotlib.org/stable/users/explain/colors/colormaps.html>, 2023. Accessed: 2023-09-25.
- [67] C. Turkay, A. Lundervold, A. Lundervold, and H. Hauser. Representative factor generation for the interactive visual analysis of high-dimensional data. *IEEE Trans Vis Comput Graph*, 18(12):2621–2630, 2012. doi: 10.1109/tvcg.2012.256
- [68] S. van den Elzen, D. Holten, J. Blaas, and J. J. van Wijk. Reducing snapshots to points: A visual analytics approach to dynamic network exploration. *IEEE Trans Vis Comput Graph*, 22(1):1–10, 2016. doi: 10.1109/TVCG.2015.2468078
- [69] C. van Onzenoodt, P.-P. Vázquez, and T. Ropinski. Out of the plane: Flower vs. star glyphs to support high-dimensional exploration in two-dimensional embeddings. *IEEE Trans Vis Comput Graph*, pp. 1–15, 2022 (early access). doi: 10.1109/TVCG.2022.3216919
- [70] P. Virtanen, R. Gommers, T. E. Oliphant, M. Haberland, et al. SciPy 1.0: Fundamental algorithms for scientific computing in Python. *Nat Methods*, 17:261–272, 2020. doi: 10.1038/s41592-020-0772-5
- [71] T. von Landesberger, M. Gerner, and T. Schreck. Visual analysis of graphs with multiple connected components. In *Proc. VAST*, pp. 155–162, 2009. doi: 10.1109/vast.2009.5333893
- [72] K. H. Wapman, S. Zhang, A. Clauset, and D. B. Larremore. Quantifying hierarchy and dynamics in US faculty hiring and retention. *Nature*, 610(7930):120–127, 2022. doi: 10.1038/s41586-022-05222-x
- [73] M. Waskom. seaborn.swarmplot. <https://seaborn.pydata.org/generated/seaborn.swarmplot.html>, 2016. Accessed: 2022-12-27.
- [74] M. L. Waskom. seaborn: statistical data visualization. *J Open Source Softw*, 6(60):3021, 2021. doi: 10.21105/joss.03021
- [75] Z. Wu, S. Pan, F. Chen, G. Long, C. Zhang, and S. Y. Philip. A comprehensive survey on graph neural networks. *IEEE Trans Neural Netw Learn Syst*, 32(1):4–24, 2021. doi: 10.1109/tnnls.2020.2978386
- [76] C. Ying, T. Cai, S. Luo, S. Zheng, G. Ke, D. He, Y. Shen, and T.-Y. Liu. Do transformers really perform badly for graph representation? In *Proc. NeurIPS*, vol. 34, pp. 28877–28888, 2021. doi: 10.48550/arXiv.2106.05234
- [77] Z. Zang, S. Cheng, L. Lu, H. Xia, L. Li, Y. Sun, Y. Xu, L. Shang, B. Sun, and S. Z. Li. EVNet: An explainable deep network for dimension reduction. *IEEE Trans Vis Comput Graph*, pp. 1–18, 2022 (early access). doi: 10.1109/TVCG.2022.3223399
- [78] D. Zhang, J. Yin, X. Zhu, and C. Zhang. Network representation learning: A survey. *IEEE Trans Big Data*, 6(1):3–28, 2018. doi: 10.1109/TBDATA.2018.2850013
- [79] F. Zhou, J. Li, W. Huang, Y. Zhao, X. Yuan, X. Liang, and Y. Shi. Dimension reconstruction for visual exploration of subspace clusters in high-dimensional data. In *Proc. PacificVis*, pp. 128–135, 2016. doi: 10.1109/pacificvis.2016.7465260
- [80] H. Zou and T. Hastie. Regularization and variable selection via the elastic net. *J R Stat Soc Series B Stat Methodol*, 67(2):301–320, 2005. doi: 10.1111/j.1467-9868.2005.00503.x
- [81] H. Zou, T. Hastie, and R. Tibshirani. Sparse principal component analysis. *J Comput Graph Stat*, 15(2):265–286, 2006. doi: 10.1198/106186006X113430
- [82] J. Y. Zou, D. J. Hsu, D. C. Parkes, and R. P. Adams. Contrastive learning using spectral methods. *Proc. NIPS*, 26, 2013.